Int. J. Electrochem. Sci., 16 **(2021)** Article Number: 211042, doi: 10.20964/2021.10.46

International Journal of
ELECTROCHEMICAL
SCIENCE
www.electrochemsci.org

Effect of Mercury(II) Ions on the Corrosion Resistance of Aluminium Alloy Coatings in 3.5% wt. NaCl solution

Xiong Chen[1,*], *Yanming Xia*[2], *Fang Zhuang*[1], *Zhao Liu*[1], *Zhiming Gao*[2,*]

[1] Petrochina Jiangsu LNG Company Limited, Nantong, 226001, China
[2] Engineering Research Center of Composite and Functional Materials, School of Materials Science and Engineering, Tianjin University, Tianjin, 300072, China
[*] E-mail: chenxiong@petrochina.com.cn; gaozhiming@tju.edu.cn

Received: 2 July 2021 / *Accepted:* 17 August 2021 / *Published:* 10 September 2021

In order to investigate the influence of mercury ions (Hg^{2+}) on the corrosion behavior of typical materials used in open rack vaporizer (ORV) in solutions containing chloride ions, 5052 aluminum alloy substrate flame sprayed with aluminum-zinc coating was used as a research object. The electrochemical corrosion behavior of the coating in 3.5% wt. NaCl solutions containing different concentrations of Hg^{2+} was investigated by potentiodynamic polarization and electrochemical impedance spectroscopy (EIS) techniques, and the surface microstructure and physical phases of the coating were characterized by scanning electron microscopy (SEM) and XRD. It was found that a relatively dense corrosion product film was generated on the surface of the coating in the low concentration of Hg^{2+} solution during immersion, which slightly inhibited the corrosion of the coating, at which point the self-corrosion current density was maintained at less than 10 $\mu A \cdot cm^{-2}$. While the concentration exceeded 0.5 ug/L, the corrosion rate of the coating was accelerated as the concentration increased, and the self-corrosion current density reached 23.3 $\mu A \cdot cm^{-2}$ at the Hg^{2+} concentration of 30 ug/L. After 32 days of immersion, a higher R_t value of the sample in the low concentration of mercury ion solution can reach 13205.8 $\Omega \cdot cm^2$, which is only 2627.3 $\Omega \cdot cm^2$ at a high concentration of 30 ug/L mercury ion, indicating that the high concentration of mercury ion under prolonged immersion produces significant damage to the corrosion resistance of the specimens. During this period, pitting holes and local coating flaking appeared on the coating surface, and the corrosion morphology changed from uniform corrosion to local corrosion.

Keywords: Aluminum alloy coating; heavy metal ions; electrochemical impedance spectrum; microstructure

1. INTRODUCTION

The open rack vaporizer (ORV) is a heat exchanger that uses seawater to heat and gasify liquefied natural gas (LNG), which is one of the key pieces of equipment in a receiving station due to its simple

operation and low operating costs. The heat transfer substrate of ORV is aluminum alloy. Due to their light weight, high thermal conductivity, excellent formability, and excellent corrosion resistance, aluminum and its alloys are widely used in aerospace and energy chemical industries, becoming an important alternative material in manufacturing heat exchange systems and chemical processing equipment [1-5], but because of the wide range of applications of aluminum alloys, they are exposed to a variety of aggressive media, and aluminum alloys are prone to corrosion in corrosive environments such as wet, acidic and alkaline [6-9]. The marine environment, as a complex environment with high salt, high humidity, rich in microorganisms and acidic, can cause pitting and uniform corrosion of the passive film on the surface of aluminum alloys [10-12], destroying the integrity of the surface passive film and causing serious degradation of marine structures such as bridges, pipelines, ships and offshore equipment [13]. Therefore, the study of the corrosion behavior of aluminum and its alloys has received much attention from scholars. At the same time, due to the pollution of the marine environment, the content of heavy metal ions in seawater has increased, which has become one of the important factors affecting the corrosion of aluminum alloy equipment.

Researches on the effects of metal ions such as Fe^{2+}, Cu^{2+}, and Cd^{2+} on the corrosion phenomena of aluminum alloys in various environments have been carried out [14-16]. Bessone [17] et al. achieved the tracking of surface processes by measuring the open circuit potential-time response of pure aluminum (99.99%) in mercury(II) acetate solutions of different concentrations and pH and combining scanning microscopy as well as EDAX / X-ray analysis, and found that Hg^{2+} ions can be directly reduced on bare aluminum after aluminum immersion, forming a direct contact between metals and triggering surface diffusion, which allows the formation of amalgam. The aluminum atoms diffuse through the liquid mercury and oxidize at the amalgam/electrolyte interface, destroying the aluminum surface oxide film and eroding the substrate in the process. Pawel [18], Leeper [19] and Pojtanabuntoeng [20] et al. summarized the effects of mercury monomers, mercury ions and organic mercury compounds on the corrosion of aluminum alloys, copper alloys, stainless steel and carbon steel, and found that the corrosion types due to the replacement and reduction of the mercury ions and the formation of mercury monomers include amalgamation, amalgamation corrosion, galvanic coupling corrosion, liquid metal embrittlement, and in general a variety of corrosion acting together on aluminum equipment, causing fracture of aluminum equipment.

Although there have been many studies on the effect of heavy metal ions on the corrosion resistance of aluminum, the materials used are mostly pure aluminum or aluminum alloys after grinding and polishing in the available studies, while in practical applications to protect or mitigate the corrosion process, protective coatings are usually applied to the metal surface [21-24], and paints and metal coatings, among others, can protect the structure from corrosion in a lasting way [25-27] . Therefore, exploring the corrosion behavior of aluminum coatings in seawater containing heavy metal ions is of great importance for the promotion of aluminum applications and the further development of marine equipment. In this project, 5052 aluminum alloy, which is common in 5XXX [28-30] series aluminum alloys, was used and aluminum-zinc alloy coating with lower chemical potential was thermally sprayed on its surface with a thickness of about 300 μm. When corrosion and wear occurred, the coating provided anti-corrosion current to the base metal, thus preventing corrosion of the base material. By setting up electrochemical experiments with typical ORV materials, the influence of mercury ions (Hg^{2+}) in 3.5%

wt. NaCl solution on the corrosion behavior of aluminum alloy coating composite system is investigated, which is of guiding significance for clarifying the corrosion mechanism of Hg^{2+} on the coating and optimizing the selection of coating and sealer materials.

2. EXPERIMENTAL

2.1 Material and solution

In this experiment, the surface of 5052 aluminum alloy was coated with a layer of aluminum alloy coating similar to the composition of the substrate by flame spraying, which is a typical material used for ORV heat exchanger tubes. The aluminum alloy sheet coated with coating and sealer was machined into blocks with a working area of 15mm×15mm. The surfaces of the specimen except for the working surface were sealed with epoxy resin.

The solution used in this experiment was prepared with 3.5% wt. NaCl solution, according to the water quality requirements of the equipment operating environment in Table 1, different concentrations of Hg^{2+} ions (0.3, 0.5, 5, 15, 25, 30ug/L) were added to the solution to investigate the effect of mercury ion concentration on the corrosion resistance of the specimens in full immersion corrosion.

Table 1. Seawater quality parameters required by the manufacturer

Substances	Concentration range	Units
pH	7.5～8.5	/
Residual chlorine	＜0.5	mg/L
Suspended substances	＜80	mg/L
Copper ions	＜10	ug/L
Mercury ions	＜0.5	ug/L

2.2 Electrochemical testing

In the process of full immersion corrosion, the electrochemical impedance spectrum(EIS) and dynamic potential polarization curve of 8, 16 and 32 days of immersion was measured by using PARSTAT2273 electrochemical workstation. The traditional three-electrode system was used, where the reference electrode is saturated glycury electrode, the counter electrode is platinum sheet electrode, and the specimen with effective test area of 2.25 cm^2 is the working electrode. The open circuit potential was measured before testing the impedance spectrum. And the impedance spectrum was measured after stabilization with an amplitude of 10mV and a frequency range of 100kHz~0.01Hz, followed by a dynamic potential polarization test with a scan rate of 2 mV/s and an anodic scan range of +1000mV.

2.3 Surface analysis

The surface morphology of the specimens before and after corrosion was observed and analyzed by scanning electron microscope (su1510), and XRD physical phase analysis was performed by X-ray diffractometer (D8 ADVANCE) with a scanning angle range of 10°~120°.

2.4 Weight loss test

The weight of the specimens was measured before and after the full immersion experiment using a balance with an accuracy of 0.1 mg, each set of data was repeated three times, and the average value of the weight loss of the specimens was listed in the results to assess the service life of the coating.

3. RESULTS AND DISCUSSION

3.1 Electrochemical corrosion behavior

Fig. 1 shows the polarization curves of the coated specimens immersed in 3.5% wt. NaCl solutions containing different concentrations of Hg^{2+} for different days. The anode curves show obvious changes after immersion in different solutions, and show a slight passivation phenomenon after 8 and 16 days, while the anodes of the specimens after 32 days of immersion show active dissolution. The existence of diffusion characteristics of the anode is also caused by the hindering effect of the corrosion product film layer on the diffusion migration of metal cations. This is due to the fact that when the mercury ions in solution come into contact with the aluminum coating surface, the following reactions occur as shown in equations (1) and (2):

$$Al - 3e^- \rightarrow Al^{3+} \text{ (anodic reaction)} \quad 1)$$

$$Hg^{2+} + 2e^- \rightarrow Hg \quad 2)$$

The cathodic curves of the specimens do not differ much because oxygen absorption corrosion and hydrogen precipitation reaction mainly occur at the cathode, and the hydrogen precipitation reaction dominates, as shown in the following equations (3) and (4):

$$H_2O + 2e^- \rightarrow OH^- + 1/2H_2\uparrow \text{ (cathodic reaction)} \quad 3)$$

$$O_2 + H_2O + 4e^- \rightarrow 4OH^- \text{ (cathodic reaction)} \quad 4)$$

Furthermore, when Al^{3+} and OH^- in the solution come into contact on the surface of the coating, the following reaction occurs as shown in equation (5):

$$Al^{3+} + 3OH^- \rightarrow Al(OH)_3 \quad 5)$$

At the same time, the electrochemical reaction becomes more complicated due to the presence of dissolved oxygen in the solution, and Al_2O_3 may be generated.

The corrosion characteristic parameters including self-corrosion potential (E_{corr}), self-corrosion current density (I_{corr}) and anodic Tafel slope (B_a) can be obtained according to the polarization curve, as shown in Table 2. In 3.5% wt. NaCl solutions containing different concentrations of Hg^{2+}, the combination of both deposition of metal monomers and destruction of the passive film results in an insignificant change in the self-corrosion potential for the same immersion time, while the overall self-corrosion potential showed a slight positive shift with longer immersion time at the same concentration, which may be due to the deposition of more metal mercury replaced on the coating surface [19]. During the immersion process, the overall trend of self-corrosion current density decreases first and then increases with the increase of mercury ion concentration. At the low concentrations of 0, 0.3 and 0.5 ug/L of mercury ions, the I_{corr} always remains below 10 $\mu A \cdot cm^{-2}$ during the immersion process, indicating that the low concentration of mercury ions would reduce the corrosion rate [31]. And at the mercury ion concentration of 5 and 15 ug/L, with the extension of the immersion time, the dynamic change of the I_{corr} shows a decrease and then increase, which is related to the destruction of the passive film on the surface of the coating and the generation and dissolution process of the corrosion product film. However when the concentration of mercury ions reaches a high concentration of 25 and 30 ug/L, the I_{corr} increases gradually with time, and could reach 23.3 $\mu A \cdot cm^{-2}$ after 32 days of immersion, reflecting that the high concentration of mercury ions has a significant impact on the corrosion resistance of the coating, which is explained by reaction (2), where mercury ions resulted in the formation of galvanic couples between the mercury monomers and aluminum, where aluminum acting as the anode will be corroded [32]. In summary, the low concentration of mercury ions slows down the corrosion rate of the coating while the high concentration of mercury ions will significantly reduce the corrosion resistance of the coating.

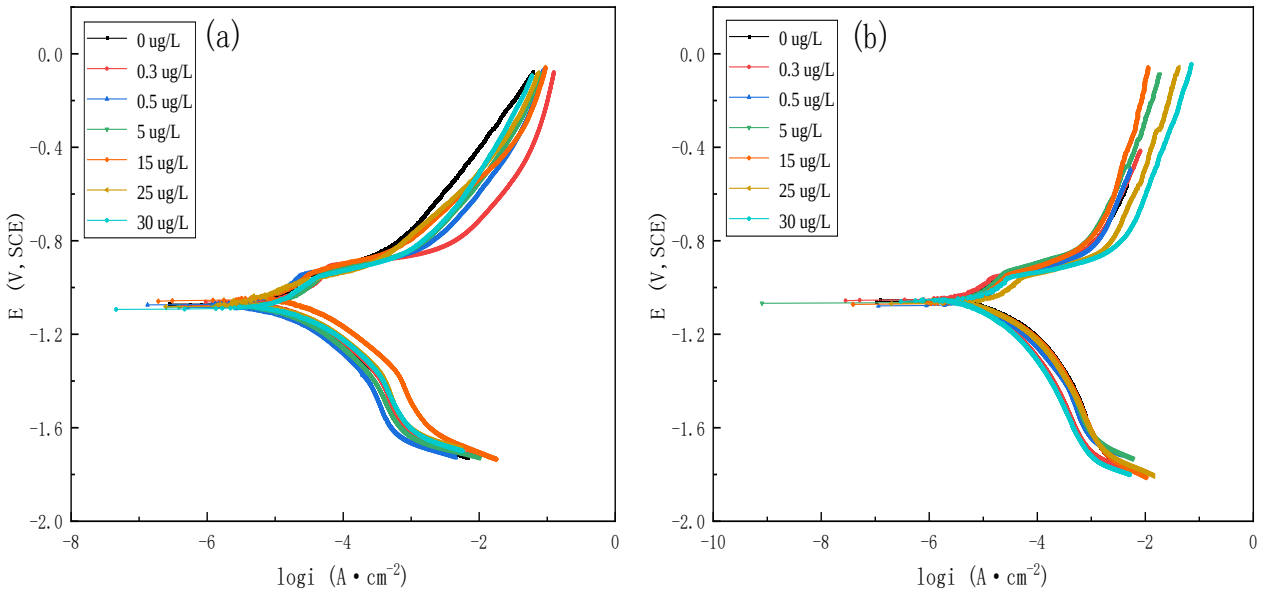

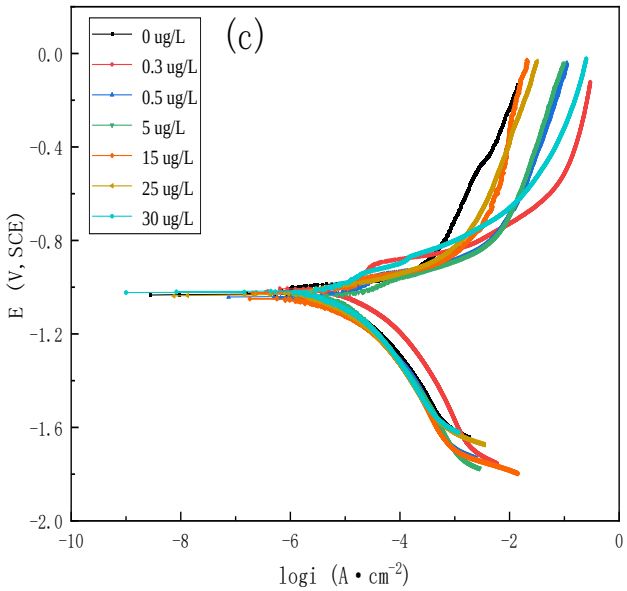

Figure 1. Polarization curves of specimens immersed in 3.5% wt. NaCl solutions with Hg^{2+} concentrations of 0 - 30 ug/L for different days: (a) 8d, (b) 16d and (c) 32d

Table 2. Polarization parameters of the coatings immersed in solutions containing mercury ions

Immersion time /d	Concentration/ ($ug \cdot L^{-1}$)	0	0.3	0.5	5	15	25	30
8	E_{corr}/(mV)	-1078	-1080	-1073	-1084	-1057	-1082	-1093
	I_{corr}/ ($\mu A \cdot cm^{-2}$)	10.05	9.563	9.984	12.13	12.37	13.54	13.31
	B_a	151	161	193	192	221	146	132
16	E_{corr}/(mV)	-1059	-1057	-1078	-1067	-1073	-1068	-1059
	I_{corr}/ ($\mu A \cdot cm^{-2}$)	8.591	7.565	7.141	8.370	10.84	12.38	13.55
	B_a	271	289	218	276	255	191	182
30	E_{corr}/(mV)	-1032	-1023	-1032	-1042	-1034	-1034	-1024
	I_{corr}/($\mu A \cdot cm^{-2}$)	9.190	8.825	7.465	11.12	12.55	19.94	23.32
	B_a	186	231	223	168	154	122	96

Note: E_{corr} (vs.SCE) / mV is the self-corrosion current density of the specimen, I_{corr} / ($\mu A \cdot cm^{-2}$) is the self-corrosion current density of the specimen, B_a / ($mV \cdot dec^{-1}$) is the anodic Tafel slope of the specimen.

To further analyze the electrochemical kinetic processes on the coating surface, the electrochemical impedance spectra (EIS) of 5052 coated specimens were tested after immersion in 3.5% wt. NaCl solutions containing different concentrations of mercury ions for different days, and the results obtained are shown in Fig. 2. Fig. 2 (a), (b) and (c) show the Nyquist and Bode plots of the specimens after 8, 16 and 32 days of immersion in different solutions, respectively. From the Nyquist plots, it can be seen that all coatings exhibit the characteristics of capacitive arc in different solutions, indicating that the electrochemical corrosion mechanism does not change. But the radius of capacitive arc resistance varies with the concentration, which decreases after the addition of mercury ions in Fig. 1 (a) and (b),

indicating that mercury ions reduce the corrosion resistance of the specimen for a short period of time. While it increases instead in the low concentration of mercury ion solution and continues to decrease in the high concentration of mercury ion solution in Fig. 1 (c), suggesting a significant decrease in corrosion resistance. Since the high and low frequency capacitive arcs partially overlap therefore a broad peak can be seen in the phase angle diagram from the Bode plot, the electrochemical process is fitted with the equivalent circuit in Fig. 3, where R_s represents the solution resistance, R_{film} and CPE_{film} represent the resistance and capacitance of the corrosion product film, R_{ct} represents the charge transfer resistance, and CPE_{dl} represents the double electric layer capacitance [33]. All capacitances in the circuit are replaced by constant phase angle elements (*CPE*) to compensate for the effects caused by the inhomogeneity of the specimen surface [34].

The resistance value of the specimen at 0.01 Hz is usually used to represent the strength of the corrosion resistance of the specimen, which are obtained by fitting the Bode plot as shown in Table 3. The results show that when the immersion time is 8 days and 16 days, the R_t value of the specimen does not change much with the concentration of mercury ions, and the value after 16 days of immersion is overall larger than that of 8 days, probably because the specimen undergoes the process of destruction of the surface oxide film after 8 days of immersion, while the corrosion product film layer with shielding effect is formed on the surface of the specimen after 16 days of immersion. After 32 days of immersion, a higher R_t value of the sample in the low concentration of mercury ion solution can reach 13205.8 $\Omega \cdot cm^2$, which indicates that the corrosion resistance of the specimen is better, corresponding to the polarization curve. In contrast, at a high concentration of 30 ug/L mercury ion, the R_t value is only 2627.3 $\Omega \cdot cm^2$, which is much lower than that in the blank solution, indicating that the high concentration of mercury ion under prolonged immersion produces significant damage to the corrosion resistance of the specimens.

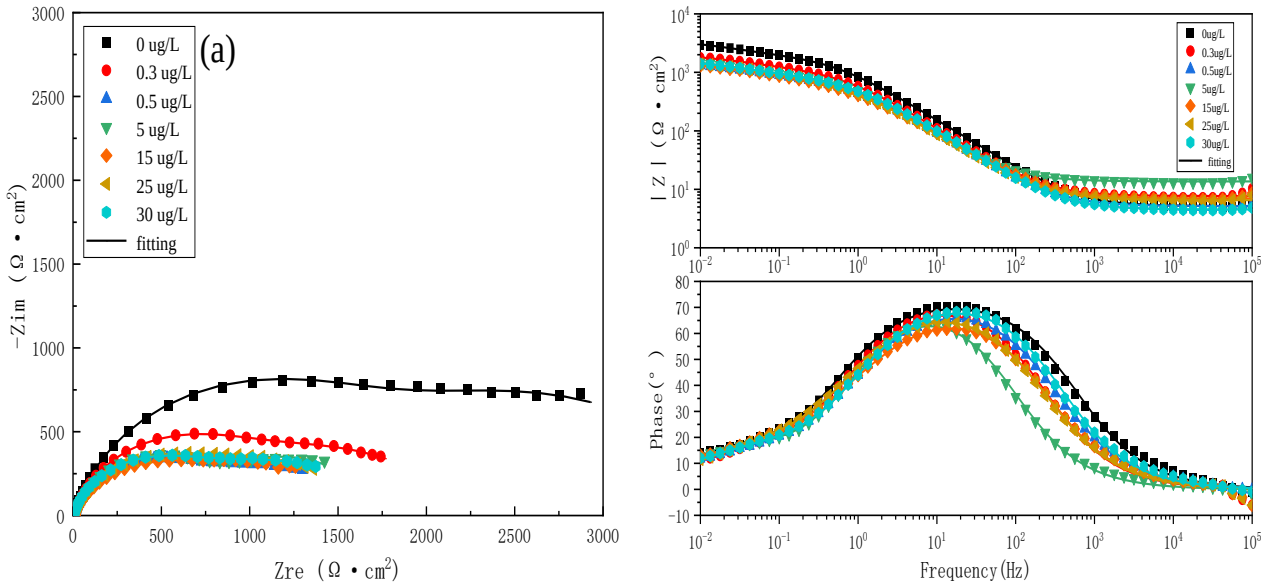

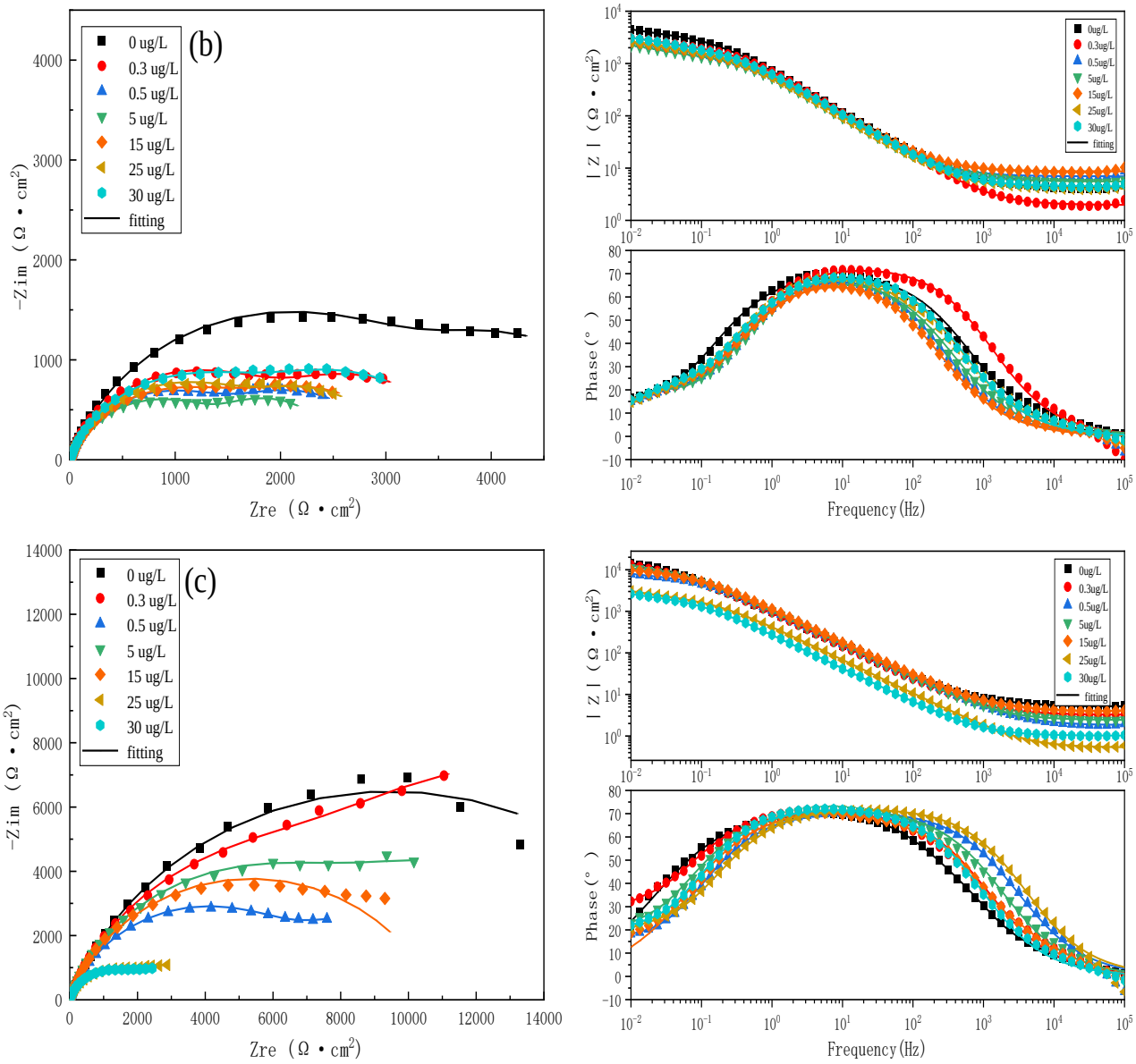

Figure 2. EIS curves of 5052 coated specimens immersed in 3.5% wt. NaCl solutions with Hg^{2+} concentrations of 0 - 30 ug/L for different days: (a) 8d, (b) 16d and (c) 32d

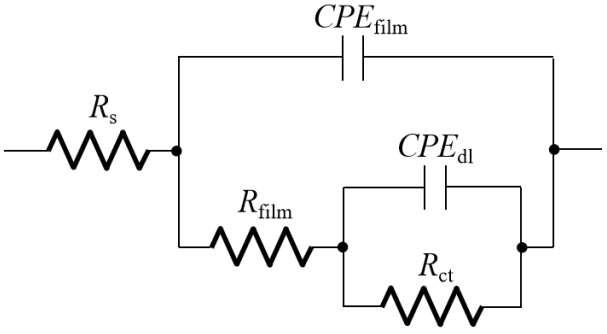

Figure 3. The equivalent circuit of 5052 coated specimens immersed in 3.5% wt. NaCl solutions with Hg^{2+} concentrations of 0 - 30 ug/L for different days

Table 3. The resistance values of specimens at 0.01Hz ($\Omega \cdot cm^2$)

$C_{Hg}^{2+}/(ug \cdot L^1)$	0	0.3	0.5	5	15	25	30
8d	3004.6	1803.2	1335.7	1452.9	1311.4	1402.6	1419.9
16d	4497.2	3114.3	2525.1	2198.0	2629.4	2633.1	3086.4
32d	14423.8	13205.8	8024.9	11069.2	9688.4	3067.9	2627.3

3.2 Microstructure of coating surface

The specimens immersed in 3.5% wt. NaCl solution containing different concentrations of mercury ions for 32 days were observed by scanning electron microscopy for microscopic morphology, and the morphology shown in Figure 4 was obtained. The coating surface remains intact after 32 days of immersion in 3.5% wt. NaCl solution without mercury ions, and white clustered corrosion products can be seen in Fig. 4(a), which were not sufficient to cover the surface completely but could plug the pores on the specimen surface and prevent further diffusion of aggressive media into the coating interior. With the addition of mercury ions to the solution, as shown in Fig. 4 (b)-(d), the low concentration of mercury ions induces the formation of a dense layer of corrosion products on the surface of the specimen, which completely covers the surface of the sample, thus acting as a shield and contributing to the improvement of the corrosion resistance of the specimen, which is consistent with the results of the EIS. And with the increase of mercury ion concentration, as more mercury monomers are deposited on the coating surface, more Al-Hg couples are formed to accelerate the corrosion process of Al anodes, and more white corrosion products can be seen continuously generated on the specimen surface. The shedding of inclusions results in a local corrosion morphology similar to pitting pits, which becomes a channel for ion diffusion and adversely affects the corrosion resistance of the specimen. When the solution contains a high concentration of mercury ions, the coating surface will still generate a large number of white corrosion products, and corrosion pits appears, in addition to large areas of specimen surface spalling similar to the phenomenon reported in the study conducted by Zhang [35], resulting in a significant decrease in corrosion resistance of the specimen, which is consistent with the electrochemical test results. In fact the mechanism of this corrosion process is similar to that described by Zhang et al [36]. In this process, chloride ions destroy the surface passive film and corrosion will preferentially sprout at surface inhomogeneities. It can be speculated that during shorter time EIS measurements, the inductive semicircle characteristics will be seen in the Nyquist diagram.

The cause of this phenomenon is not only related to the accelerating effect of galvanic corrosion, but also to the solubilization of aluminum by mercury monomers [17], and the following reactions of Eqs. (6) [19] and (7) [17] may occur when mercury is in contact with aluminum:

$$2Al(Hg) + 6H_2O \rightarrow 2Al(OH)_3 + 3H_2\uparrow + 2(Hg) \quad (6)$$

$$2Al(Hg) + 6H_2O \rightarrow Al_2O_3 \cdot 3H_2O + 3H_2\uparrow + 2(Hg) \quad (7)$$

Where the Hg monomers play a catalyst-like role and continuously cause the dissolution of aluminum, while the generated hydrogen bubbles also contribute to the coating peeling [17], thus

accelerating the destruction of the coating, which was also reported by Chu [37] during studies of the corrosion of magnesium alloys.

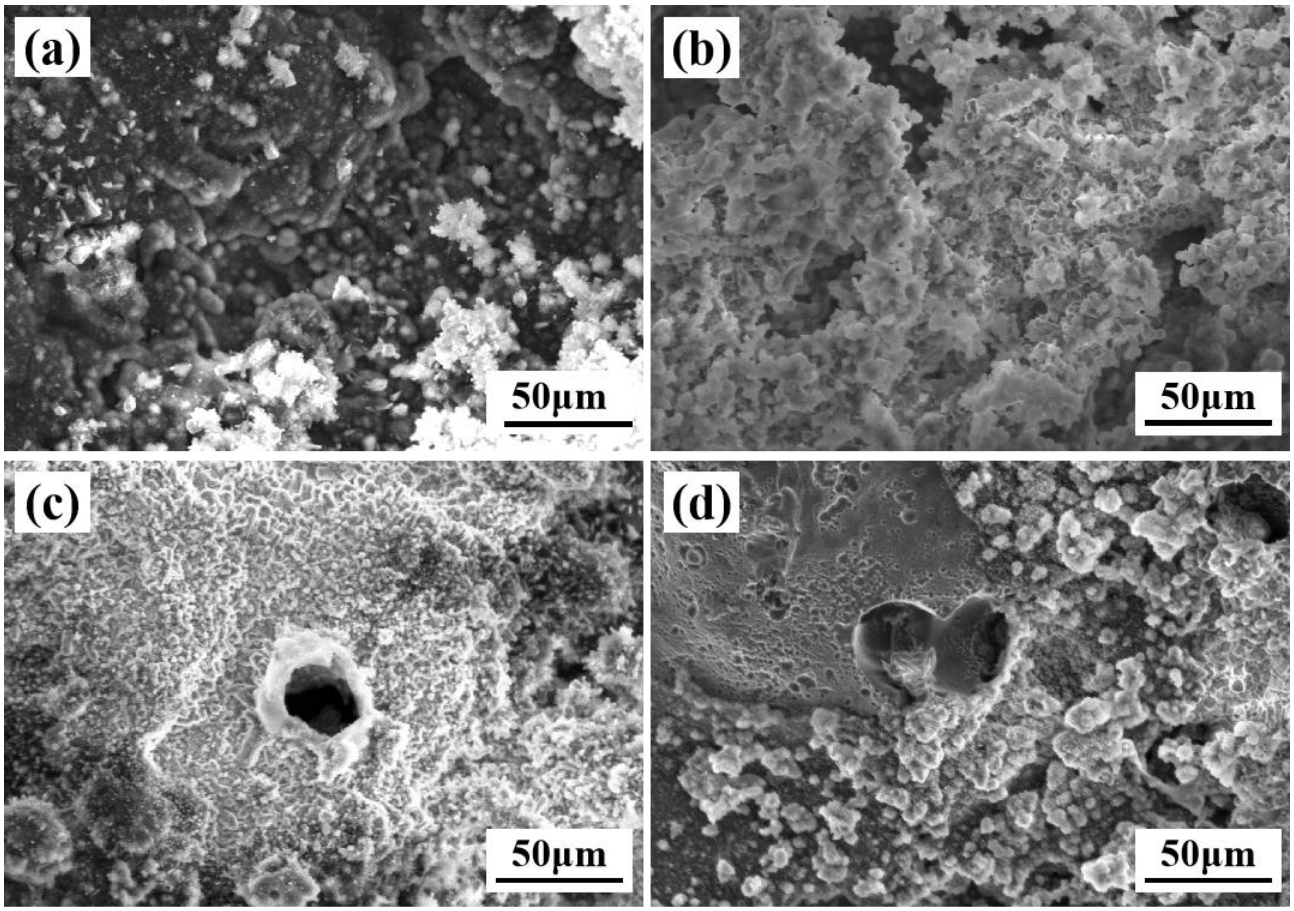

Figure 4. SEM images of the coatings after 32 days of immersion in 3.5% wt. NaCl solution containing different concentrations of mercury ions: (a) 0 ug/L, (b) 0.3 ug/L, (c) 15 ug/L and (d) 30 ug/L

To further investigate the composition of the corrosion products, the surface XRD analysis of the coatings immersed in 3.5% wt. NaCl solutions containing different concentrations of mercury ions for 32 days was performed after the experiment, and the results were obtained as shown in Fig. 5. The corrosion products of the coating in different solutions are $Al(OH)_3$ and Al_2O_3, and the content of heavy metal ions in the solution does not affect the type of corrosion products. It is presumed that Al_2O_3 may come from the hydrolysis of $Al(OH)_3$ and the formation of the coating in air, the peak of $Al(OH)_3$ on the surface of the coating in high concentration mercury ion solution is more obvious, but as mentioned before this is a porous layer, the corrosion medium will penetrate into the interior of the coating and corrode the internal surface, and eventually local corrosion is formed on the surface of the coating. Due to the autocatalytic effect inside the pores, the formation of a local acidic environment, further accelerating corrosion to promote the spalling of the coating surface. The $Al(OH)_3$ product film in the low mercury ion solution is denser and can effectively play a role in preventing ion diffusion, so the corrosion rate is reduced. The peak of the Al substrate in the spectrum is very obvious, which is caused by the thin film of corrosion products and the X-ray penetration of the surface film to the substrate. The

peak of Hg is not detected from the spectrum, probably because the content of replacement deposition is too small to be detected.

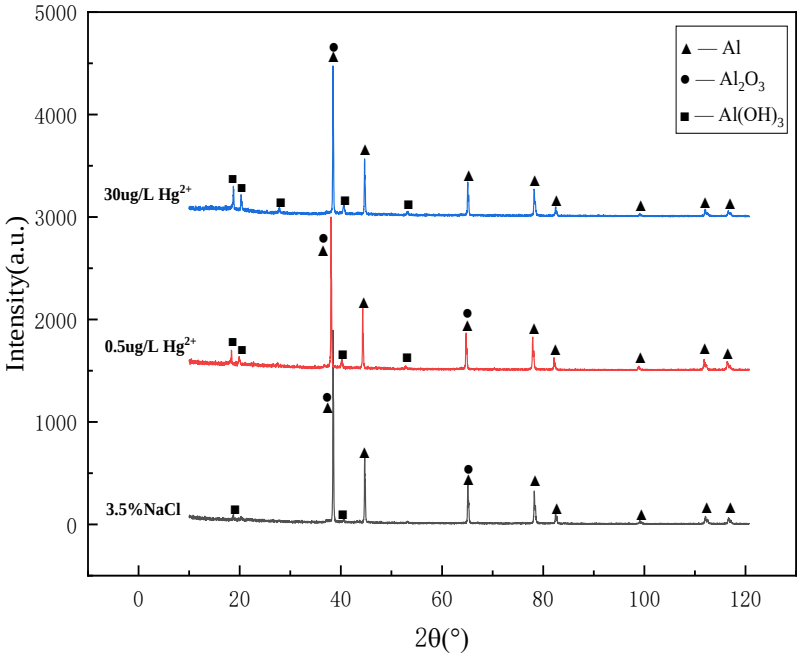

Figure 5. XRD spectrum of surface corrosion products of the coating after 32 days of immersion in 3.5% wt. NaCl solution containing Hg^{2+}

3.3 Weight loss test

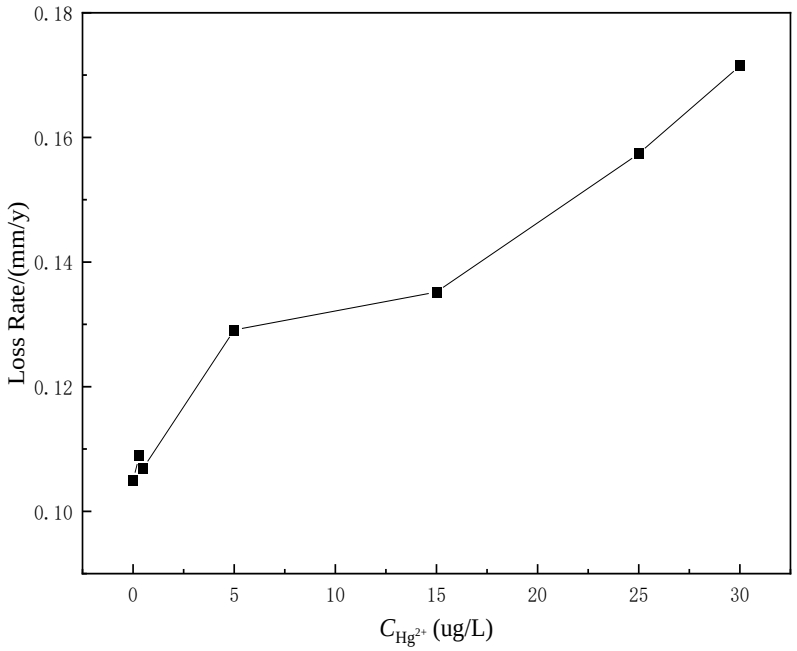

Figure 6. Weight loss curve of the specimen after 32 days of immersion in 3.5% wt. NaCl solution containing different concentrations of mercury ions

The weight loss data of the coatings in Fig. 6 were measured after the specimens soaked in 3.5% wt. NaCl solution with different mercury ion content for 32 days. The weight loss rate barely increases when the mercury ion content is trace, while it increases from 104.9 μm/y to 171.5 μm/y as the mercury ion concentration increases to 30 ug/L, which indicates that the corrosion rate of the specimen increases significantly and is consistent with the results of the preliminary electrochemical test.

In conclusion, in the process of full immersion corrosion of this coating in 3.5% wt. NaCl solution with different concentrations of mercury ions, it is proved that the concentration of mercury ions above 0.5 ug/L will have a more obvious effect on the corrosion resistance of the coating, while the concentration of mercury ions in the actual application of 5052 coated aluminum alloy pipeline in seawater is much lower than this value, which is in line with the Japanese manufacturer Sumitomo regulations for Hg^{2+} in seawater quality requirements (Table 1). Therefore, the coating initially meets the actual engineering requirements and has the prospect of further promotion and development.

4. CONCLUSION

1) The concentration of mercury ions has a significant effect on the full immersion corrosion behavior of 5052 aluminum alloy coating in 3.5% wt. NaCl solution, the corrosion rate will be slow down at low concentration of mercury ions, while the corrosion process of the coating will be significantly accelerated at high concentration of mercury ions, mainly due to the destruction of aluminum by mercury monomers formed by mercury ion replacement.

2) A uniform corrosion morphology can be observed on the surface of the coating when the concentration of mercury ions is low, and a relatively dense layer of corrosion products film formed on the surface, playing a certain role in shielding. While the mercury ion concentration is higher, pitting corrosion occurs and the phenomenon of large area peeling appears on the surface of the coating. In solutions with different mercury ion content, the corrosion products on the surface of the coating are of the same type, but the densities of the corrosion product films are different.

3) The thinning rate increases from 104.9 μm/y to 171.5 μm/y, suggesting a decrease in corrosion resistance and a shortened service life. According to the above analysis, with a thickness of 300 μm, the operating life of the coating is about three years in a qualified environment.

ACKNOWLEDGEMENTS
This work was supported by Research on ORV Corrosion Mechanism and Application of Prevention and Control Technology (2019-XSKJ-04), Tianjin Science and Technology Project (No.20YDTPJC01780), and Shandong Taishan Industry Leading Talents Project (No.SF1503302301).

References

1. Z. Zhang, Z.L. Xu, J. Sun, M.T. Zhu, Q. Yao, D.J. Zhang, B.W. Zhang, K. Xiao and J.S. Wu, *Int. J. Electrochem. Sci.*, 15 (2020) 1218.
2. G.A. Zhang, L.Y. Xu and Y.F. Cheng, *Corros. Sci.*, 51 (2009) 283.
3. W.J. Qi, X. Qi, B. Sun, C. Wan, J.R. Jin and R.G. Song, *Mater. Perform.*, 56 (11) (2017) 58.
4. J.C. Williams and E.A. Starke Jr., *Acta Mater.*, 51 (19) (2003) 5775.
5. Y.P. Xiao, Q.L. Pan, W.B. Li, X.Y. Liu and Y.B. He, *Mater. Des.*, 32 (4) (2011) 2149.
6. P. Priputen, M. Palcut, M. Babinec, J. Mišík, I. Černičková and J. Janovec, *J. Mater. Eng.*

Perform., 26 (8) (2017) 3970.
7. M. Palcut, P. Priputen, M. Kusý and J. Janovec, *Corros. Sci.*, 75 (2013) 461.
8. M. Palcut, L. Ďuriška, M. Špoták, M. Vrbovský, Ž. Gerhátová, I. Černičková and J. Janovec, *J. Min. Metall. Sect. B.*, 53 (3) (2017) 333.
9. J.L. Ma, J.B. Wen, Q.A. Li and Q. Zhang, *Int. J. Hydrogen Energy*, 38 (34) (2013) 14896.
10. Z. Szklarska-Smialowska, *Corros. Sci.*, 41 (9) (1999) 1743.
11. F. Deflorian, S. Rossi and S. Prosseda, *Mater. Des.*, 27 (9) (2006) 758.
12. L.P. Tian, X.H. Zhao, Y. Zuo, J.M. Zhao and J.P. Xiong, *Mater. Chem. Phys.*, 104 (1) (2007) 24.
13. Q.J. Zhu, K. Wang, X.H. Wang and B.R. Hou, *Surf. Eng.*, 28 (4) (2014) 300.
14. M.G.A. Khedr, *J. Electrochem. Soc.*, 136 (4) (1989) 968.
15. T. Xu, Z.F. Hu and C. Yao, *Int. J. Electrochem. Sci.*, 14 (3) (2019) 2606.
16. X.J. Raj and N. Rajendran, *J. Fail. Anal. Prev.*, 19 (1) (2019) 250.
17. J.B. Bessone, *Corros. Sci.*, 48 (12) (2006) 4243.
18. S.J. Pawel and E.T. Manneschmidt, *J. Nucl. Mater.*, 318 (2003) 355.
19. J.E. Leeper, *Energy Process/Canada*, 73 (1981) 46.
20. T. Pojtanabuntoeng, C. Saiwan, S. Sutthiruangwong and D.L. Gallup, *Corros. Eng. Sci. Technol.*, 46 (4) (2011) 547.
21. D.P. Zeng, Z.Y. Liu, S. Bai and J. Wang, *Coatings*, 9 (12) (2019) 867.
22. Y.S. Tao, T.Y. Xiong, S. Chao, L.Y. Kong, C.Y. Cui, T.F. Li and G.L. Song, *Corros. Sci.*, 52 (10) (2010) 3191.
23. R.M.H.P. Rodriguez, R.S.C. Paredes, S.H. Wido and A. Calixto, *Surf. Coat. Technol.*, 202 (1) (2007) 172.
24. Y. Wan, H. Wang, Y.D. Zhang, X.M. Wang and Y.B. Li, *Int. J. Electrochem. Sci.*, 13 (2) (2018) 2175.
25. W.B. Choi, L. Li, V. Luzin, R. Neiser, T.G. Herold, H.J. Prask, S. Sampath and A. Gouldstone, *Acta Mater.*, 55 (3) (2007) 857.
26. D. Zhang, P.H. Shipway and D.G. Mccartney, *J. Therm. Spray Technol.*, 14 (1) (2005) 109.
27. P.C. King and M. Jahedi, *Appl. Surf. Sci.* 256 (6) (2010) 1735.
28. S. Shamsudeen and E.R.D. John, *Mater. Perform. Charact.*, 8 (4) (2019) 555.
29. S. Gudić1, L. Vrsalović, M. Kliškić, I. Jerković, A. Radonić and M. Zekić. *Int. J. Electrochem. Sci.*, 11 (2) (2016) 998.
30. D. Zerouali, Z. Derriche and M.Y. Azri, *J. Appl. Sci.*, 6 (11) (2006) 2491.
31. H.F. Wang, J.L. Wang, W.W. Song, D.W. Zuo and D.L. Shao, *Int. J. Electrochem. Sci.*, 11 (2016) 6933.
32. X.H. Wang, Z.W. Peng, L. Ma, Y.H. Lin, G.X. Li and H.L. Wang, *Int. J. Electrochem. Sci.*, 12 (2017) 11006.
33. H.X. Chen and D.J. Kong, *Mater. Chem. Phys.*, 251 (2020) 123200.
34. J.D. Zuo, B. Wu, C.Y. Luo, B.Q. Dong and F. Xing, *Corros. Sci.*, 152 (2019) 120.
35. K. Zhang, B.W. Wen, L.W. Zhang, C. Li, J. Liu and P. Yi, *Int. J. Electrochem. Sci.*, 15 (2020) 11036.
36. X.G. Zhang, X. Liu, W.P. Dong, G.K. Hu, P. Yi, Y.H. Huang and K. Xiao, *Int. J. Electrochem. Sci.*, 13 (2018) 10470.
37. P.W. Chu, E.L. Mire and E.A. Marquis, *Corros. Sci.*, 128 (2017) 253.